Sensors & Transducers, Vol. 239, Issue 12, December 2019, pp. 17-33

www.sensorsportal.com

Sensors & Transducers

Published by IFSA Publishing, S. L., 2019
http://www.sensorsportal.com

Rapid Detection of Pesticide Residues in Vegetables and Fruits via a Hand-Held Instrument

[1, 2, 3, *] Wenping Zhao, [1] Hui Zhang, [1] Zhaoqiang Shi, [1, 2, 3] Yemin Guo, and [1, 2, 3] Xia Sun

[1] School of Agriculture Engineering and Food Science, Shandong University of Technology, No. 266 Xincun West Road, Zhangdian District, Zibo City, 255000, Shandong Province, P.R. China
[2] Shandong Provincial Engineering Research Center of Vegetable Safety and Quality Traceability, No. 266 Xincun West Road, Zhangdian District, Zibo City, 255000, Shandong Province, P.R. China
[3] Zibo City Key Laboratory of Agricultural Product Safety Traceability, No. 266 Xincun West Road, Zhangdian District, Zibo City, 255000, Shandong Province, P.R. China
[1] Tel.: +86-533-2786558, fax: +86-533-2786558
[*] E-mail: 187286528@qq.com

Received: 6 November 2019 /Accepted: 30 November 2019 /Published: 1 December 2019

Abstract: A hand-held instrument for the rapid detection of pesticide residues in vegetables and fruits that was based on acetylcholinesterase (AChE) screen-printed carbon electrode (SPCE) was developed. This device integrated a printable enzyme-based biosensing system and a weak current signal detection circuit. This instrument was coupled with a compact electronic interface for electrochemical detection and real-time wireless data transmission to an internet device. The measurement principle for measuring the pesticide concentration was based on the enzyme inhibition method. The SPCE biosensor was inserted directly into the hand-held instrument to detect pesticides on-site. This biosensor showed a wide linear range for detecting organophosphorus pesticides, extending from 0.05 to 1×10^5 μg/L, with a detection limit of 0.05 μg/L. The recovery rate for organophosphorus pesticides in vegetables was 89.3 %-103.3 %, and the relative standard deviation was 3.45 %-5.43 %; therefore, the prepared sensor showed good repeatability and stability, and it provided a reliable method for the rapid and real-time detection of organophosphorus pesticide residue.

Keywords: AChE biosensor, Hand-held instrument, Rapid detection, Pesticide residues, Screen-printed carbon electrode.

1. Introduction

Pesticides help to increase the production of high-quality fruits and vegetables by controlling the spread of pests during growth [1-2]. The benefits that pesticides bring to the global food supply are not in doubt, but their incorrect application can harm human health [3]. Therefore, it is necessary to investigate the pesticides in these products to identify residues and quantify their levels. In this context, there is a growing need for rapid and more efficient methods for analyzing pesticide residues in food as the demand for residue-free foodstuffs increases [4].

Traditional pesticide residue detection methods include chromatography (including gas chromatography, liquid chromatography and capillary

electrophoresis), spectroscopy (including spectrophotometry, molecular fluorescence spectroscopy, and Raman spectroscopy), immunoassays, and chemical methods [5-8]. Although these methods are highly accurate and highly sensitive, the required pretreatment is tedious and the equipment is expensive [9-13]. These approaches require professional staff to operate in addition to a long analysis time, which is not conducive to field monitoring and promotion [14-15]. Therefore, there is an urgent need to develop a low-cost and reliable hand-held instrument for the rapid detection of organophosphate pesticides [16].

It is universally acknowledged that the rapid determination of pesticide residues is performed by enzyme inhibition method, biosensor, immunoassay, in vivo detection and other methods [17-18]. Among these, the enzyme inhibition method is relatively mature, and it is the most widely used technique for rapid testing [19-22].

The AChE biosensor has gradually replaced these traditional methods for pesticide residue determination because of its simplicity, high speed, high selectivity and low relative cost [23-24]. In recent years, detection and analyses based on AChE and its inhibitors have been widely used in food, environmental monitoring and other fields [25-26]. After several years of continuous research, the sensitivity, stability and accuracy of the AChE biosensor have been greatly improved, but the following issues must still to be solved:

(1) They largely consist of three ordinary electrodes, and they are inconvenient to carry.

(2) They still require sample pretreatment by centrifugation, ultrasound and other means, which is not conducive to rapid on-site detection.

(3) Their on-site detection data cannot be uploaded to the internet database synchronously, which leads to gaps in the reliability and effectiveness of the traceability system.

Based on research about key biosensor technologies, we have developed a hand-held instrument for the rapid detection of pesticide residues in vegetables and fruits based on AChE SPCE. This device has integrated a printable enzyme-based biosensing system and a weak current signal detection circuit. It was coupled with a compact electronic interface for electrochemical detection and real-time wireless data transmission to an internet device. The measurement principle for detecting the pesticide concentration was based on the enzyme-inhibition method. The SPCE biosensor was inserted directly into the hand-held instrument to detect pesticides on-site, and this biosensor showed a broad linear range for the detection of organophosphorus pesticides. The combination of micro-detection instruments and rapid detection methods supports the possibility of rapidly detecting pesticide residues in fruits and vegetables at any time and in any place.

2. Experiments

The production of the detection instrument is divided into two parts, with one on the production of the enzyme biosensor, including the modification of nanometer materials on the surface of the SPCE and the immobilization of AChE. The second part involves the development of an instrument for the rapid detection of pesticide residues based on enzyme biosensors, including the primary controller module, detection module, power supply module, display and print module and wireless transmission module.

2.1. Preparation of Enzyme Biosensor based on SPCE

2.1.1. Preparation Method for Enzyme Biosensor based on SPCE

First, this project employed a MWCNTs-SnO_2-CHIT compound to form a nanocomposite film with good redox activity and biocompatibility on the electrode surface, which amplified the current response of the sensor (Fig. 1). Second, the AChE on the electrode surface could be strongly modified by sol gel method. Finally, Nafion was added to prevent the spread of AChE.

1) Synthesis of the MWCNTs-SnO_2-CHIT compound.

A 0.1 g portion of CHIT was added to 50 ml of acetic acid solution at a 1% concentration to make a CHIT solution with a concentration of 0.2 %, and then the CHIT was completely dissolved by magnetic stirring for more than 8 hours. The SnO_2: MWCNTs at a mass ratio of 1:3 was dispersed in the 0.2 % CHIT solution. Stable black dispersions were obtained by ultrasonic dispersion for 6 hours at room temperature. The resulting highly dispersed black suspensions were MWCNTs-SnO_2-CHIT compounds.

2) Preparation of the Nafion/AChE/MWCNTs-SnO_2-CHIT/SPCE sensor.

A 2.5 μL MWCNTs-SnO_2-CHIT compound suspension was added to the pretreated SPCE surface to obtain MWCNTs-SnO2-CHIT/SPCE after drying naturally in the air. Next, 2.5 μL of 0.1 U/μL AChE was applied to the MWCNTs-SnO_2-CHIT/SPCE surface, and AChE/MWCNTs-SnO_2-CHIT/SPCE was obtained after drying at 4 °C. Finally, 2.5 μL of Nafion solution at a 0.5 % concentration was applied to the AChE/MWCNTs-SnO_2-CHIT/SPCE surface and air-dried. The electrode surface was then cleaned with pH 7.5 phosphate-buffered saline, and the unbound AChE was removed. Following nitrogen drying, the Nafion/AChE/MWCNTs-SnO_2-CHIT/SPCE electrode was obtained. The assembly process is shown in Fig. 2. The prepared electrode was stored at a temperature of 4 °C in a dry environment.

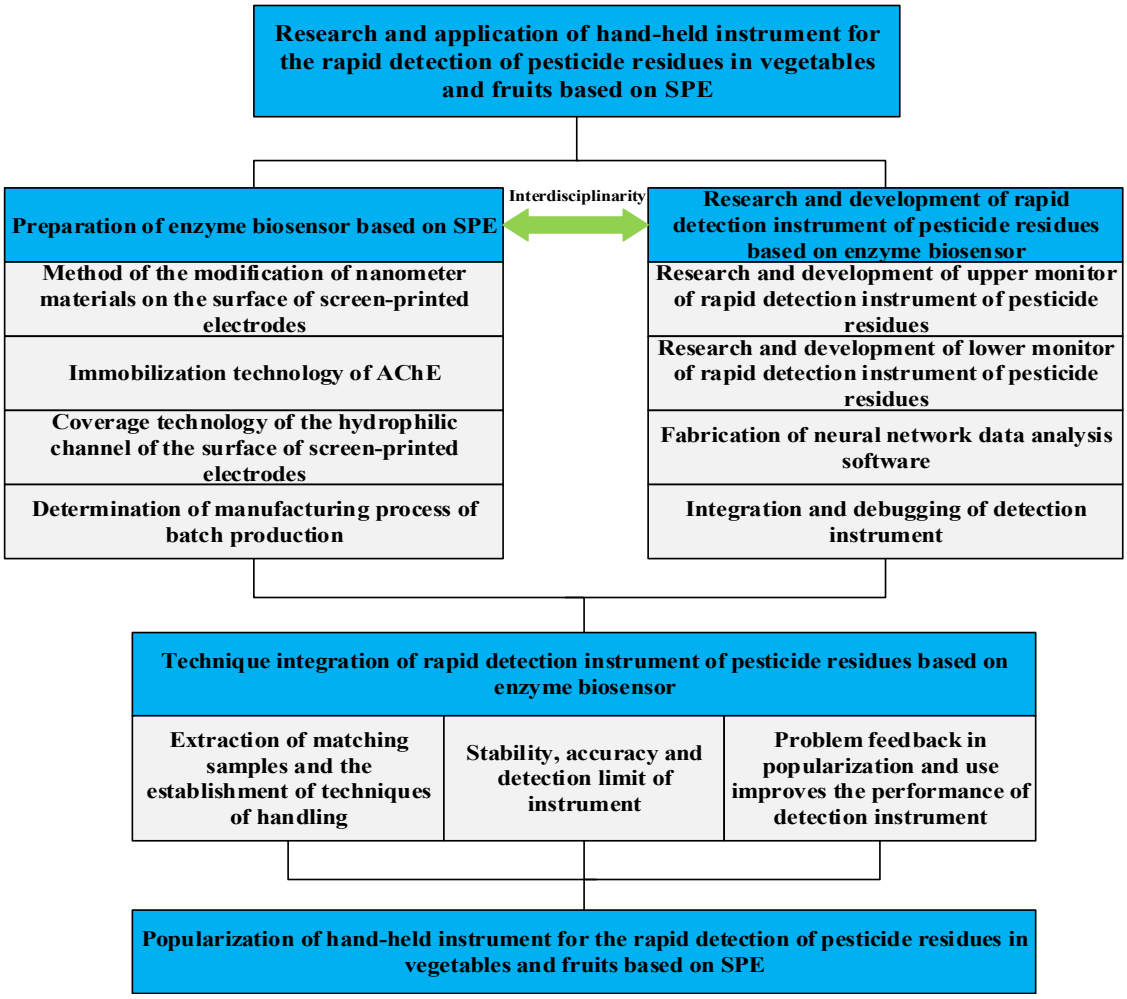

Fig. 1. Research and development scheme of this project.
(Materials: multi-walled carbon nanotubes (MWCNTs), chitosan (CHIT), SnO_2, Nafion, SPCE, AChE, vegetables and fruits, standard concentrations of pesticides, and phosphate-buffered saline. Methods: enzyme inhibition method and sol gel method. pH: 7.5. Scan rate: 0.05 V/s. Temperature condition: room temperature).

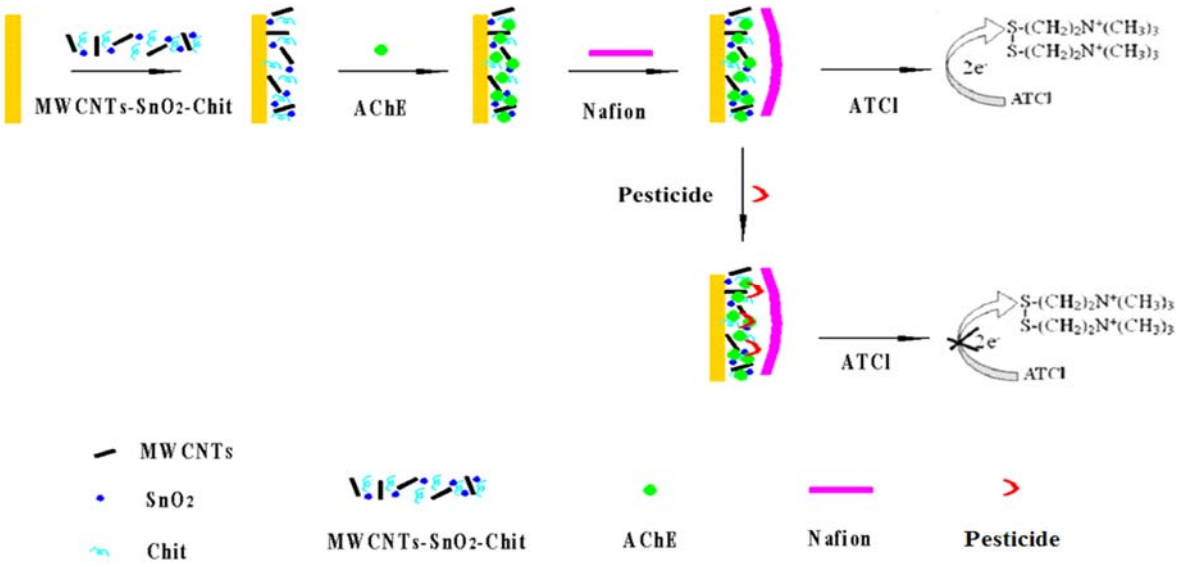

Fig. 2. Assembly process for the Nafion/AChE/MWCNTs-SnO_2-CHIT/SPCE sensor.
(Materials: MWCNTs, CHIT, SnO_2, Nafion, SPCE, AChE, vegetables and fruits, standard concentrations of pesticides, and phosphate-buffered saline. Methods: enzyme-inhibition method and sol gel method. pH: 7.5. Scan rate: 0.05 V/s. Temperature condition: room temperature).

2.1.2. Reaction Principles for AChE and Pesticide

The basic unit of AChE is a tetramer consisting of subunits, each of which has a molecular weight of 3.2×105 u (1 u=166×10^{-27} kg) and an active center. The active center contains two or more two-amino acid residues and an ester exchange site consisting of a serine and a histidine residue. AChE catalyzes the substrate of acetylcholine and hydrolyzes it into an electroactive substance, such as choline and acetic acid. Organophosphate pesticides can imitate the action of acetylcholine and AChE, the serine active site of acidified AChE, and consequently, it influences the production of phosphorylated AChE. Its hydrolysis rate is relatively slow. This compound cannot recover the enzyme activity, and it will contribute to a decrease or loss in enzyme activity. The amount of electroactive substances will be reduced, and the measured current will also be smaller, as shown in Fig. 3. Based on a large number of experiments, a linear regression equation between the suppression and pesticide concentration was established to measure the pesticide content [10]. The lower monitor of the pesticide residue detection instrument in this paper is based on this principle. The monitor collects changes in electric current before and after pesticide inhibition by the circuit and then obtains the pesticide concentration. Therefore, it is necessary to study the preparation method for the AChE biosensor, which produces a weak current, before developing the lower monitor in this instrument.

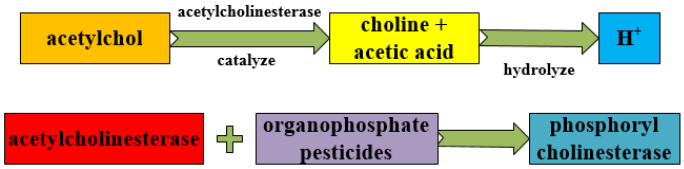

Fig. 3. Reaction principles of AChE and pesticide.

2.1.3. Relationship between the Inhibition Rate, Inhibition Time and Pesticide Concentration

1) Calculation of the pesticide inhibition rate.

The formula used to express the pesticide inhibition rate is as follows:

$$\text{Inhibition rate} = (I_0\text{-}I_1)/I_0\times 100\%.$$

I0 and I1 refer to the response current magnitude in cyclic voltammetry from the inhibitions occurring 15 minutes before and after the addition of pesticides.

2) Relationship between the inhibition rate and inhibition time.

The inhibition time is the AChE-pesticide reaction time. We used 1 μg/L chlorpyrifos as an example, as shown in Fig. 4. As the inhibition time increased, the inhibition rate increased first and then leveled off. The inhibition rate was basically stable at 15 minutes. The inhibition rate was less than 100 %, probably because the binding sites of the pesticides and enzymes have reached saturation. Therefore, 15 minutes was the optimum reaction time for chlorpyrifos suppression.

3) Relationship test between the inhibition rates of chlorpyrifos and the pesticide residues.

Fig. 5 shows the current rate of change in chlorpyrifos at different concentrations as modified by the electrode surface. With the increasing chlorpyrifos concentration, the rate of change for the current increases gradually. As shown in Fig. 6, different concentrations of chlorpyrifos have different inhibitory rates on AChE. Under optimum conditions, chlorpyrifos has a good linear relationship with the inhibition rate of pesticides over the concentration range from 5×10^{-2} to 1×10^{5} μg/L. The linear equation is y=5.2396x +6.1584. The correlation coefficient is 0.9911. The detection limit of the enzyme sensor is 0.05 μg/L.

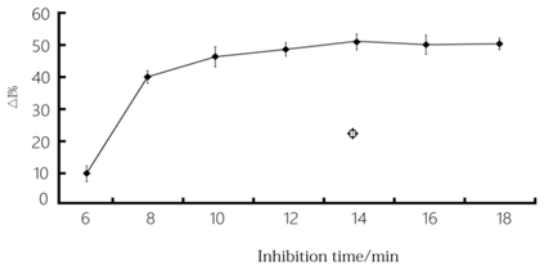

Fig. 4. Relationship between the inhibition rate and the inhibition time. (Materials: MWCNTs, CHIT, SnO_2, Nafion, SPCE, AChE, vegetables and fruits, standard concentrations of pesticides, and phosphate-buffered saline. Methods: enzyme-inhibition method and sol gel method. pH: 7.5. Scan rate: 0.05 V/s. Temperature condition: room temperature).

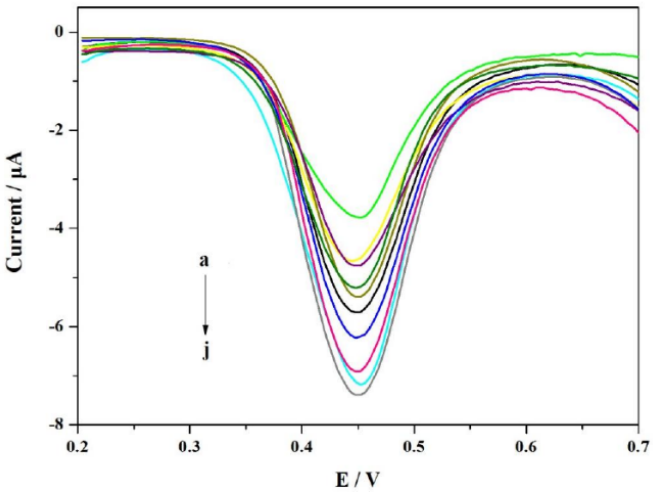

Fig. 5. Effect of the pesticide concentration on the current change in the enzyme sensor at (a) 1×10^5 μg/L; (b) 1×10^3 g/L; (c) 5×10^2 μg/L; (d) 2×10^2 μg/L; (e) 1×10^2 μg/L; (f) 10 μg/L; (g) 5 μg/L; (h) 1 μg/L; (i) 0.5 μg/L; and (j) 0.05 μg/L. (Materials: MWCNTs, CHIT, SnO_2, Nafion, SPCE, AChE, vegetables and fruits, standard concentrations of pesticides, and phosphate-buffered saline. Methods: enzyme-inhibition method and sol gel method. pH: 7.5. Scan rate: 0.05 V/s. Temperature condition: room temperature).

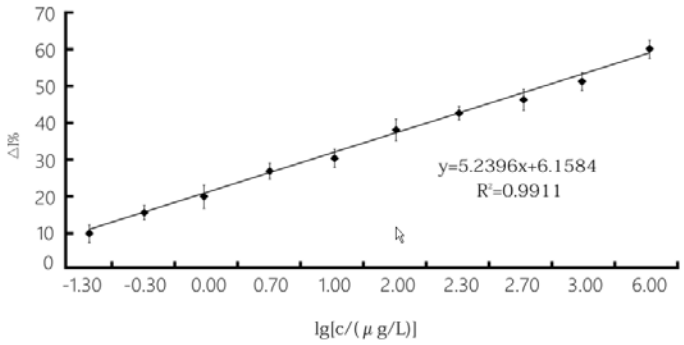

Fig. 6. Relationship between the inhibition rate and the chlorpyrifos concentration. (Materials: MWCNTs, CHIT, SnO_2, Nafion, SPCE, AChE, vegetables and fruits, standard concentrations of pesticides, and phosphate-buffered saline. Methods: enzyme-inhibition method and sol gel method. pH: 7.5. Scan rate: 0.05 V/s. Temperature condition: room temperature).

2.2. Research and Development on a Rapid Detection Instrument for Pesticide Residues based on Enzyme Biosensors

2.2.1. Primary Controller Module

The primary controller module of this project employs an STM32F100C8T6 microprocessor. To achieve the expected function of the pesticide residue detection instrument in this research, that is, the collection of weak electric signals and the conversion of analog signals into digital signals, the LCD screen displays the detection status and implements the instrument operations, detecting data prints, outputs and stores, and the lower computer transmits data wirelessly. Finally, the peripheral circuit of the minimum microprocessor system is the display interface circuit, the printer circuit, the data wireless transceiver circuit and the A/D sampling circuit. (Fig. 7).

2.2.2. Detection Module

The circuit detection process consists of events in which the constant potential circuit provides the enzyme electrode with an operating voltage of 0.5 V, the enzyme electrode reacts with the sample under analysis, and after a certain lag period (approximately 5 ~ 10 seconds), a weak current signal is produced, which ranges from several hundred nA to several μA. This weak signal is first transformed into a voltage signal after I-V conversion, the output voltage range of which can run from 0 to 5 V after the power-line interference and noise are filtered through the low pass filter. Finally, the signal enters the A/D conversion chip for A/D conversion, as shown in Fig. 8.

1) Constant potential circuit design.

For the three-electrode system, only a polarization current is provided to the electrode, and it does not affect the working electrode. The reference electrode that provides constant potential does not participate in

the reaction, and thus voltage stability is ensured. The regulation of the constant potential is achieved by the negative feedback of deep voltage. An operational amplifier (integrated components or discrete components) is used to perform calculations in which the potential difference (UWE-URE) between the operating electrode and the reference electrode is strictly equal to the input reference voltage U_0.

Owing to the fact that the operational amplifier has a high open-loop gain, it can achieve very high constant voltage accuracy; conversely, the response time of the operational amplifier is very short, and thus the regulation process of the constant potential is very fast. When the reference signal U0 is not a DC constant voltage but is a function of time, as with square, triangular, and sinusoidal voltage, the working electrode potential will vary according to the reference signal due to the fast response of the amplifier, and the UWE-URE=U_0 can still be maintained.

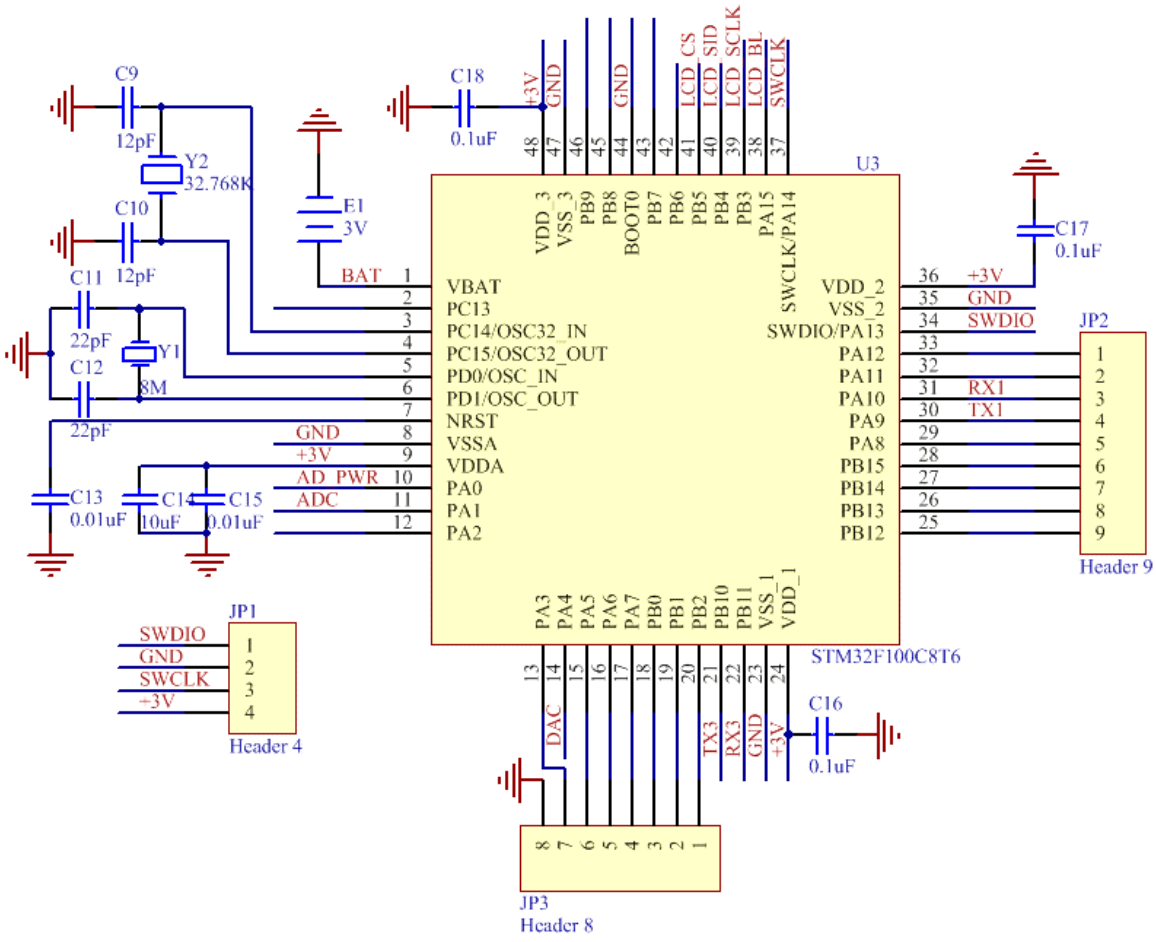

Fig. 7. STM32F103VET6 Microcontroller.

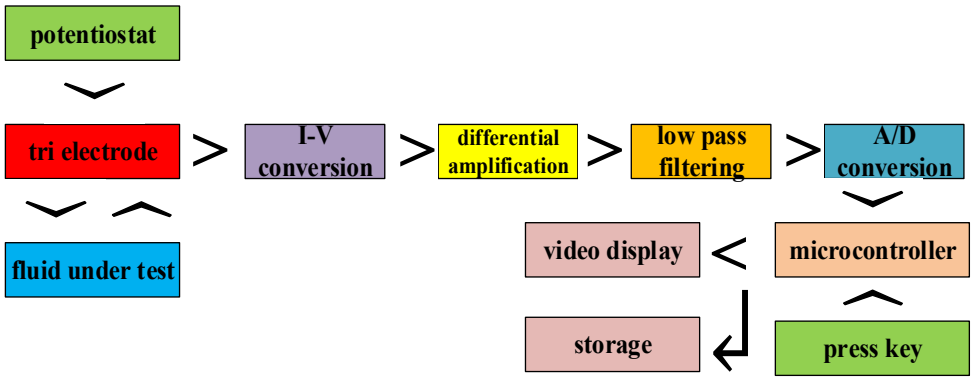

Fig. 8. Detection circuit system.

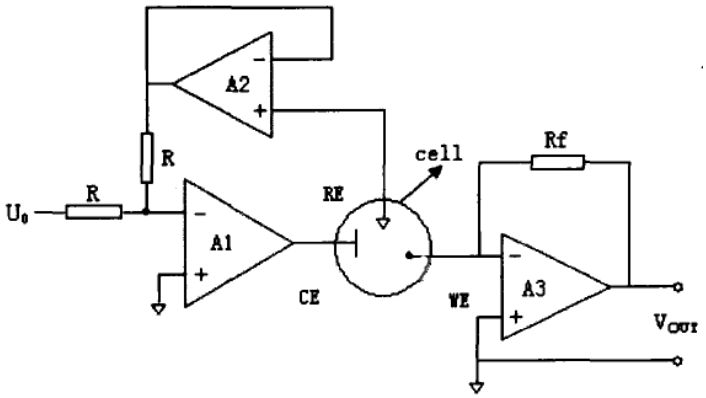

Fig. 9. Function diagram of the potentiostat.

Liquid supplied by 500 mV of constant pressure can be detected using the potentiostat principle for maintaining constant potential differences between the working electrode and the reference electrode. To regulate the constant potential, an operational amplifier with low noise, high open loop gain, high input impedance and high common mode rejection ratio is needed (Fig. 9).

In this system, an amplifier is connected to three electrodes to form a three-electrode system. The three electrodes contact the liquid and detect a weak current, and then the current is transmitted to the other circuit system through the amplifier and the working electrode. The TLC272 input of the U10 is connected to the three-terminal precision potentiometer R46, which is powered by a single supply at +5 V. The voltage on the working electrode is controlled by R4, R44 and R46, and the voltage is a constant 500 mV. Therefore, stable reaction conditions are provided for the electrochemical reaction. The following diagram in Fig. 10 shows a constant circuit.

Owing to the fact that the enzyme electrode biosensor needs a constant voltage circuit to offer a stable working voltage during its operation, the enzyme electrode in this experiment must receive 500 mV in working voltage. This design adopts the principle of partial pressure in series resistance. As shown in Fig. 10, the R46 is a precision resistor. One pin of it is connected to a voltage follower. The 500 mV voltage is obtained by the R46 (10K) potentiometer. The drive capability is increased by connecting the output to a follower circuit.

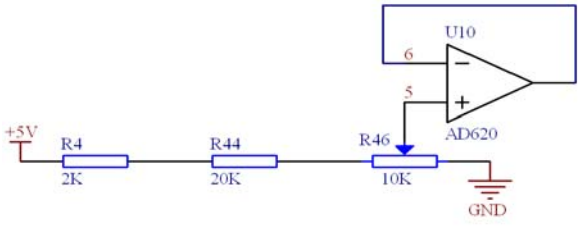

Fig. 10. Constant potential circuit.

2) Three-electrode system.

As shown in Fig. 11, the TLC272 dual operational amplifier is used here. Its internal pin 3 and pin 5 are positive inputs, the pin 2 and pin 6 are negative inputs, and the pin 1 and pin 7 are double outputs. The pin 6 connects to the pin 7; therefore, the U10A is a voltage follower, the U10A is an I-V conversion circuit, the feedback resistance is 1 MΩ, and the current-limiting resistance of the output is 100 K. The pin 6 of the U10B is connected to the pin 3 of U10A, and the pin 5 of the U10B is connected to the constant potential circuit, and thus the voltage of the pin 6 of the U10B is always the same as that of the pin 3 of the U10A. According to the circuitous philosophy of the virtual short circuit breaking line, the voltage of the pin 2 for the U10A is consistent with the voltage of the pin 3 of the U10A, so the voltage on the working electrode is always 500 mV on the pin 5 of the U10B, and it can remain unchanged to perform the function of the potentiostatic electrochemical test.

3) I-V circuit design.

The enzyme electrode reacts with the solution to produce the measured current. First, the current is converted into a voltage signal through the I-V transform, and then voltage signals in the Volt class are produced after amplification and filtering to process the AD conversion. Because the measured signals are extremely weak, the preamplifier I-V converter must have low noise characteristics and high signal-to-noise ratio output characteristics.

The microcurrent signal source can be regarded as a current source with overwhelmingly large internal resistance. A microcurrent-measuring circuit with an earth terminal is actually a microcurrent-to-voltage converter. The principle is shown in Fig. 12. For the ideal amplifier with an infinite input impedance and amplification factor, the relation between the input and output is as follows:

$$V_0 = -I_i \times R_f$$

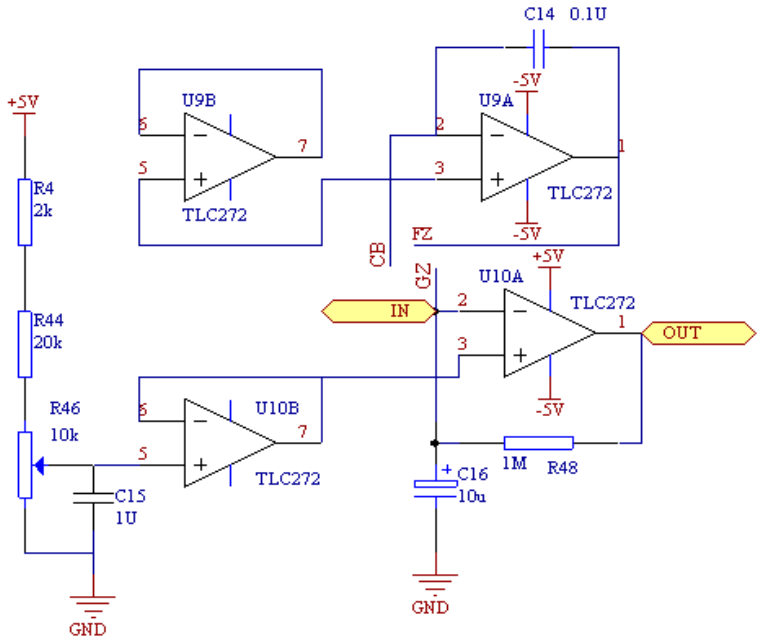

Fig. 11. Three-electrode system.

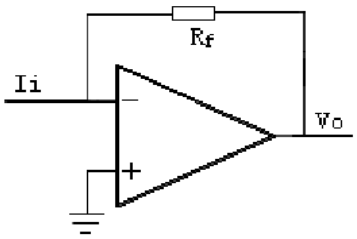

Fig. 12. Basic I-V conversion circuit.

4) Calculation of design parameters for the filter circuit.

The current signals produced by the enzyme electrode reaction after the I-V conversion circuit and the differential amplifier circuit produce noise signals of varying degrees. To detect a microcurrent, the noise interference is strongly suppressed. The signals can be collected effectively just by restraining the influence of the interference signals on the detected signals. The primary interference signal of this system is the 50 Hz power frequency signal, and thus the designed filter circuit is a low-pass filter. The signals above 50 Hz are removed, so the cut-off frequency is at least 50 Hz.

This system adopts the second-order active low-pass filter circuit and selects the AD620 operational amplifier as shown in Fig. 13.

The weak current produced by the reaction of the enzyme electrode and the liquid under analysis receives 0~4 V passing through I/V conversion and differential amplification circuit processing. Therefore, this part of the circuit is primarily for filtering. Considering the characteristics of the microcurrent signal measured by this system, the designed filter circuit has a cut-off frequency of f=50 Hz, and it can withstand a cut-off frequency of 50 Hz and only filter a 50 Hz power frequency signal and noise over 50 Hz. If the cut-off frequency is reduced, the filtered range of noise wave frequencies is larger and the influence is minimized. In addition, when the Q value is equal to 0.707, the amplitude frequency response of the low-pass filter is the most stable, and the value of resistance R and capacitance C can be calculated at this time. Because capacitors are normally only valued within a nominal value range, the value of the capacitor is usually selected first, and then the value of R is calculated. A Butterworth function and a Chebyshev function were used. The cut-off frequency is calculated by using the highly applicable Butterworth function, and the cut-off frequency of the circuit is $f0=1/(2\pi RC)$ (R6= R7= R, C9= C10= C). Provided that the capacitance is C= 0.1 μg and R=50 kΩ, the cut-off frequency is $f=1/(2\pi RC) = 31.8$ Hz. If C=0.1 μF and R=50 KΩ, the 104 ceramic capacitor and the 50 KΩ metal film resistor can be used. In this manner, low-pass filtering can be implemented, especially when filtering 50 Hz and above.

When the AD620 is open (that is, the pin 1 and the pin 8 are suspended), magnifying factor A is 1. Thus, a filter circuit is a voltage follower. In this system, second-order smoothing is added to the parts of the differential amplification section. The two filtering waves are matched with one another to filter out the signal noise, which greatly reduces the influence of the circuit noise. During the actual selection of resistance, when there is no corresponding value for the resistance, it is possible to use the resistance near this value.

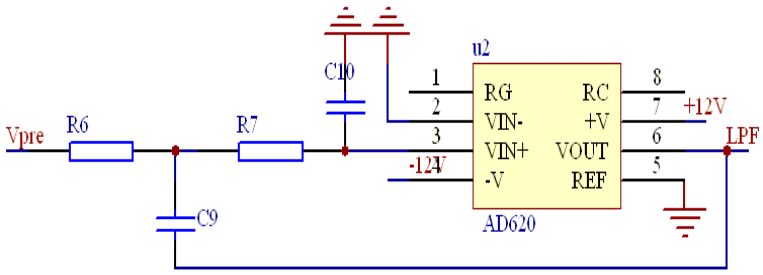

Fig. 13. Schematic diagram of an active two-order low-pass filter circuit.

5) A/D sampling.

The weak electric current signals pass through a differential amplifier circuit and the second-order active low-pass filter circuit and then form analog electrical signals. Finally, the A/D converter samples the filtered analog signals and converts them into digital signals, which are processed by a microcontroller system. This system uses a MAX187 serial 12 bit analog-digital converter. Fig. 14 shows a schematic diagram of the A/D conversion of the system.

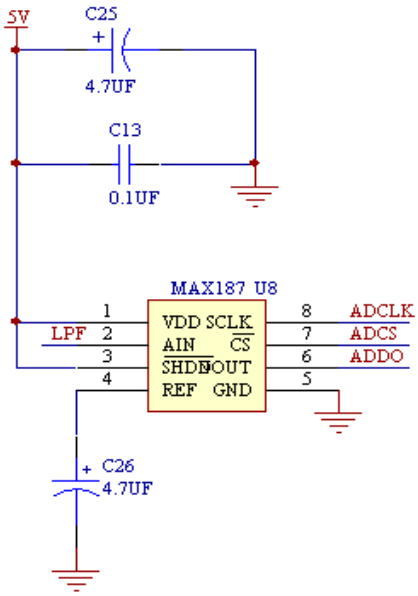

Fig. 14. Schematic diagram of A/D conversion circuit.

In Fig. 14, MAX187 from pin 2 receives the input analog signal. Pin 6 is the analog output signal. Pin 7 is the chip select signal. A low level is effective. The entire chip works at a voltage of +5 V. C26 provides the reference voltage for the chip.

2.2.3. Power Supply Module

For the detection system, good and bad power supply circuit designs will directly affect the performance because the noise generated by the external interference source can interfere with the detection circuit through the power supply circuit. Additionally, the voltage source module itself is also a source of interference. The power supply circuit is usually composed of a power transformer, rectifier circuit, filter circuit and voltage stabilizing circuit. If the output waveform of the power rectifier is not ideal, the power output will have power-line interference and other noise interference in the power line.

To eliminate the possible effects of these unnecessary factors on the system, this design adopts a three-way switching power supply produced by Shenzhen Hetian's prestigious Electronics Co., Ltd. The outputs of the positive and negative power supplies are asymmetrical. The enlargement factor of the I-V conversion circuit is very high, and the feedback resistance is great (Fig.15). The operational amplifier requires a high symmetry of positive and negative power supplies. The voltage of the IC chip used in the design of the circuit is ±5 V. The IC chip employs the WS78L05 and WS79L05 terminal regulator triodes r, and it transforms the direct current outputted by the bridge rectifier into ±5 V.

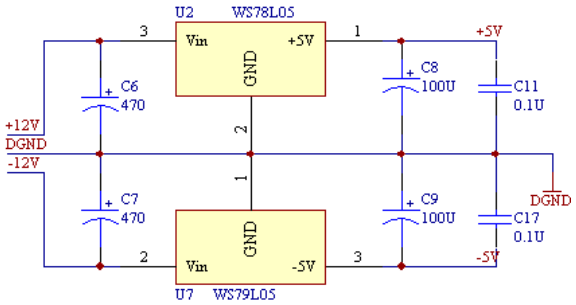

Fig. 15. Power supply circuit.

2.2.4. Design of the Display Screen, Printer and Button

1) Liquid crystal display (LCD) display interface circuit.

The interface circuits of the LCD QC12864B module and STC89C52 are shown in Fig. 16. QC12864B uses parallel communication, it has a simple external circuit, and it is connected to the single chip by means of indirect connection; that is, the I/O port is directly connected to the LCD data line and the control line. Its characteristics are simple, intuitive and

easy to operate. In this circuit, the 8-bit parallel mode is used to create the correct display. The VDD is a power drive. The + 5 V single power supply can drive a display screen. The RS and RW are read/write ports. The gray level of the display screen is adjusted by a potentiometer. E is “enable”. When E=1, the signal is in chip select mode.

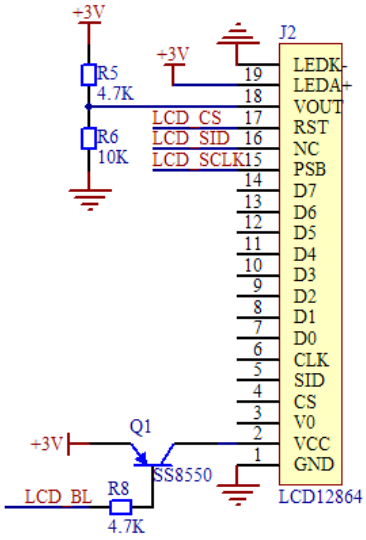

Fig. 16. Display interface circuit.

2) The circuit design of the printer.

The printer (as shown in Fig. 17) is an RD series micro-printer produced by Beijing Rongda Creative Technology Limited. The external interface of the printer is a standard parallel interface. It prints at the impact point. Its print cache is 32 K and its power supply is DC 5 V/1 A. It supports a one or two-level Chinese national character library.

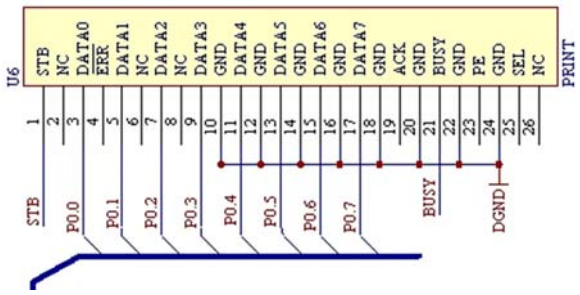

Fig. 17. Schematic diagram of the printer circuit.

The standard serial port adopts 26 lines in double needles (2.54 mm). Here, the default baud rate is 9600 BPS. The communication format used here is a serial connection asynchronous transfer format, and the logic level of the signal is at the TTL level. To connect the printer to the microcontroller, MAX3232 is needed. The microcontroller is the TTL signal level, and the printer serial port is the RS232 signal level. To connect two non-current signals, the MAX3232 transceiver is used here. The receiver in the MAX3232 converts the RS-232 signal to the TTL logic output level. In most cases, the use of a 0.1 uF shunt capacity meets the requirements. The circuit diagram of the MAX3232 transceiver is shown in Fig. 18.

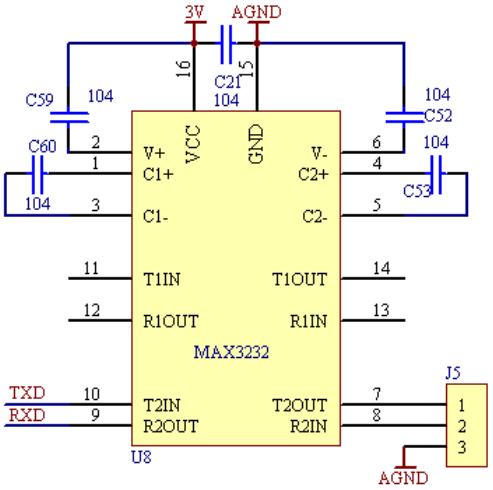

Fig. 18. Transceiver circuit.

2.2.5. Wireless Transmission Module

The wireless module uses NRF24L01, a 2.4 GHz global open ISM band (Fig. 19). Its maximum transmitting power is 0 dBm, the working voltage is 1.9~3.6 V, the rate is 2 Mbps, and no license is required. Because of the short transmission time, the collision phenomenon in wireless transmission is greatly reduced, which meets the requirements of multipoint communication and frequency hopping communications. This module is equipped with 2.4 GHz aerials of compact size. When working in reply mode, the rapid airborne transmission and boot time greatly reduce the current consumption. NRF24L01 integrates all the high-speed signal processing components associated with the RF protocol. The SPI interface of NRF24L01 can use the microcontroller's hardware SPI interface to connect to or to use the microcontroller’s I/O port for simulation. The FIFO inside it can interface with various high and low speed microprocessors, and thus it is easy to use low-cost microcontrollers.

2.2.6. The Design of the System Software

During the overall design of the application system, the software and hardware designs must be considered and developed together. When the hardware design of the system is finalized, the task of the software is clear. The software design of the system is also the design of the instrument system functions. The microcontroller software design

primarily includes the design of executive software (completing a variety of substantive functions) and the monitoring software design. The program design contains the primary program design (Fig. 21) and the subroutine design. The program design consists of a keyboard scanning subroutine, A/D conversion subroutine, display subroutine, print subroutine, and storage subroutine.

1) A/D conversion subroutine.

The A/D conversion circuit is essential to the design, and its conversion accuracy will directly affect the measurement results of the system. The following describes the MAX187 conversion subroutine.

According to the previous introduction to the MAX187 section, the mode of work is a monopole single-end internal clock mode. The program initializes the P1 port first and then writes the control word. It selects the zeroth channel, unipolar, single-ended internal clock mode. When the conversion is complete, the 12-bit conversion result is read at the DOUT port. These readings are obtained on the falling edge of each SCLK clock. Their higher four bits are saved to the 40 H, and the lower eight bits are placed in the 41 H. The following is a flowchart of the A/D conversion subroutine (Fig. 22).

2) LCD display subroutine.

A liquid crystal display program primarily displays the results from sampling the data processed by microcontroller. In this design, the liquid crystal is set to 128 × 64 dot matrix. When the 12864 LCD program is written, the time sequence is very important. However, unlike other chips, the 12864 does not have very high timing requirements (Fig. 23).

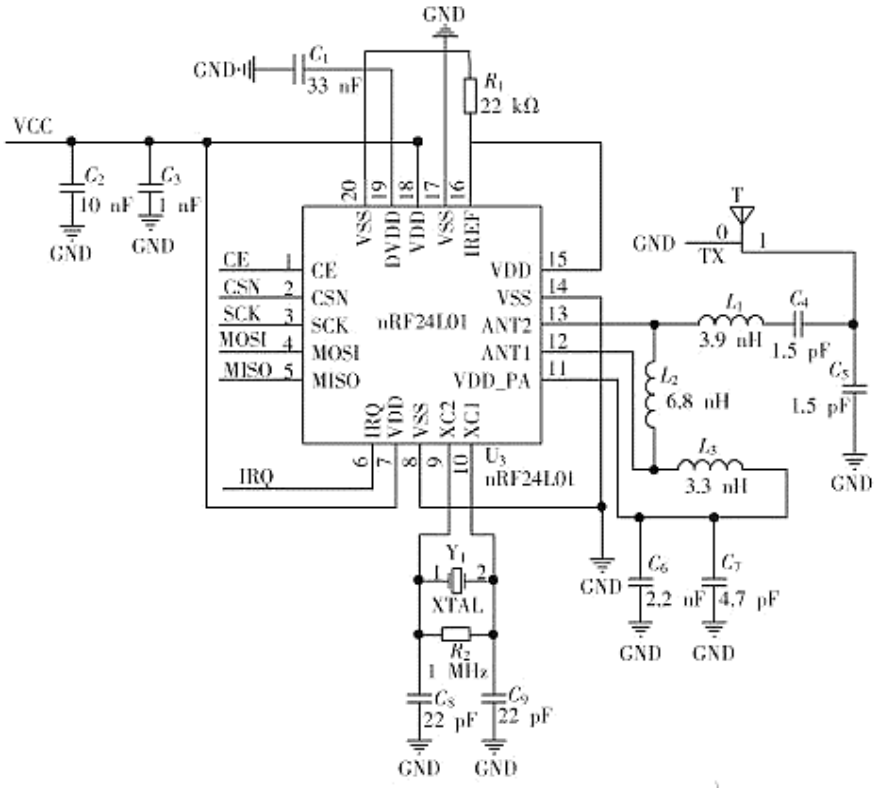

Fig. 19. NRF24L01 wireless module.



Fig. 20. Developed rapid detection system for pesticide residues based on the internet of things.

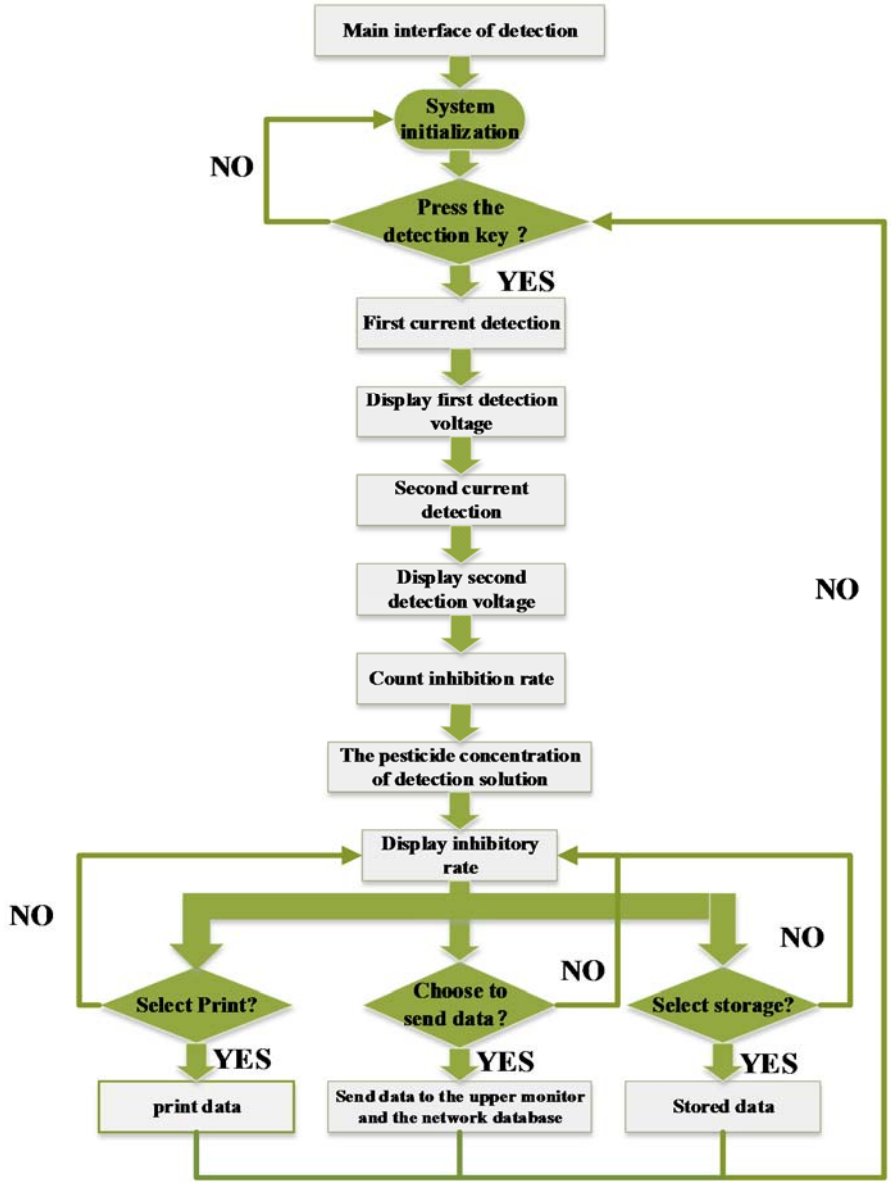

Fig. 21. Workflow chart.

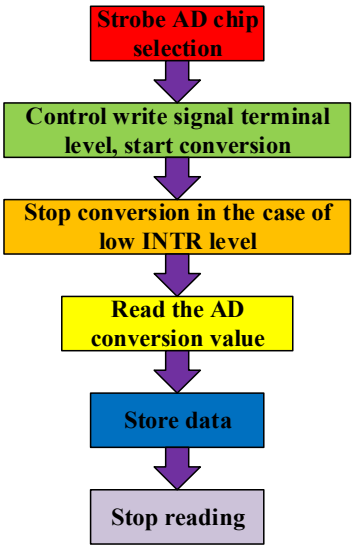

Fig. 22. Flow chart of A/D conversion subroutine.

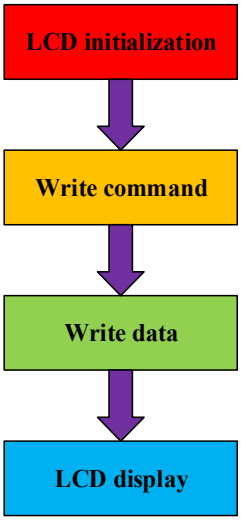

Fig. 23. Flow chart of the LCD display subroutine.

2.3. Assembly of Rapid Detection Instruments for Measuring Pesticide Residues

From the beginning of the design to the production of the complete instrument, this process must pass through several steps, including hardware design, software design, program introduction, and hardware and software debugging together. In addition, there is the appearance design of the instrument to consider, including the shell material, color selection, and the design of the operation panel.

2.3.1. Complete Instrument

The red part of the shell is made of rubber, and the black part of the shell is made of plastic, as shown in Fig. 24. The operation panel of this design is divided into a display section, a button section and a switch section. The operating part consists of 7 film buttons, which are "detection", "cancel", "confirm", "up", "down", "turn left" and "turn right". Their functions are as follows: pressing "detection" to engage the detection process, and going through the first detection and the second detection. When the detection is completed, the data are automatically saved in the additional storage. By manipulating the "direction" and "confirm" options, we can browse the data that were detected before, and "cancel" is the exit operation for such terms as "detection", "print", and "storage." The "on-off key" controls the start, initialization, and shutdown of the overall system.

3. Results and Discussion

3.1. Method of use

This instrument has the advantages of having simple operation, high accuracy and stable performance; its process and time consumption are more convenient and efficient than those reported in the literature [27]. It uses cyclic voltammetry to detect the current changes in distilled water and fruit and vegetable juice, and it uses the relationship between the current inhibition rate and the pesticide concentration to detect the concentrations of residual pesticides. The method of use is shown in Fig. 25.

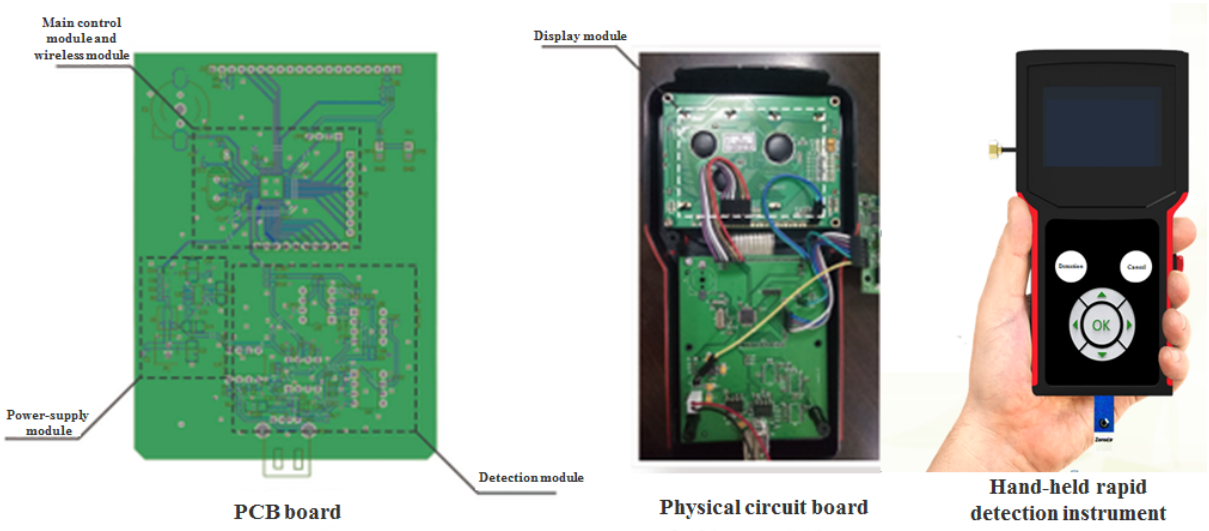

Fig. 24. Developed hand-held instrument for the rapid detection of pesticide residues.

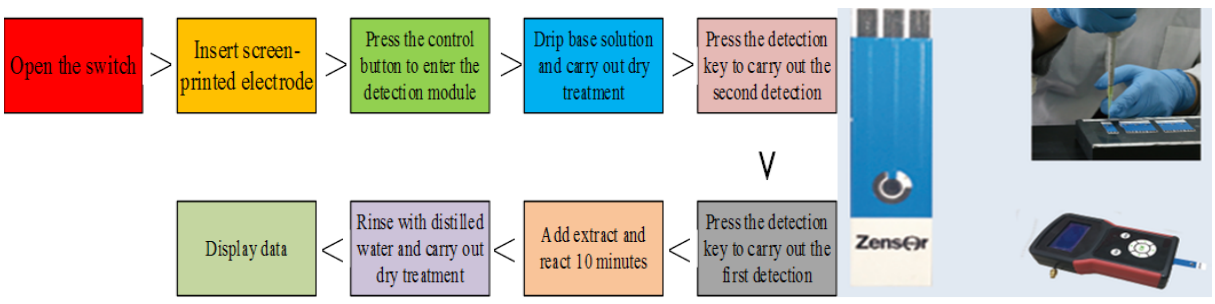

Fig. 25. Method of use.

3.2. Performance Evaluation

3.2.1. Detection Limit Range for Pesticide Residues

Under laboratory conditions, 7 groups of pesticide solutions with different concentrations were detected by this instrument. In using chlorpyrifos as an example, the concentrations were 0.02 μg/L, 0.04 μg/L, 0.05 μg/L, 0.1 μg/L, 1 μg/L, 10 μg/L, and 100 μg/L. The detection results are shown in the Table 1.

Table 1 indicates that when the concentration of pesticide residues is 0.05 μg/L, the instrument has achieved a high detection accuracy. The minimum detectable amount of pesticide residues is 0.05 μg/L. This instrument has achieved high detection accuracy relative to that reported in the literature [28]. Table 2 shows that the national standards for pesticide residues are most concentrated in the 0.1 mg/kg ~ 10 mg/kg range; therefore, the rapid detection instrument has broad application prospects and high application value.

3.2.2. Probability of Missed Samples and False Positive Rates

The NY-S12-type is can rapidly detect pesticide residues (Beijing Qiangsheng analytical instrument manufacturing center), and this instrument can detect 1000 sets of samples simultaneously. A large number of experiments show that the probability of missing the sample is ≤ 0.1 %, and the false positive rate is ≤ 2%. This result shows that the instrument has reached the preferred standard.

3.2.3. The Detection of Pesticide Residues in Real Samples

1) Processing method for test samples.

Fresh lettuce heads purchased from the supermarket were regarded as samples (the amount of pesticide residues was zero). After cleaning and drying, 5.0 g samples were collected separately and weighed accurately. A pesticide standard solution was sprayed evenly on the surface of each leaf blade. The pesticide concentrations of the samples were 1 ng/mL and 10 ng/mL. The juice from the sample was detected after air-drying.

2) Processing method of actual sample.

The fresh vegetables purchased from the supermarket are regarded as samples. Parts of the vegetables were picked, and the juice from each sample was analyzed.

3) Detection of pesticide residues in real samples.

The recovery rate of the vegetable samples was tested for this instrument, in vegetables such as cabbage, lettuce, leeks and pakchoi. As shown in Table 3, the recovery rate for these vegetables is 89.3 %-103.3 %, and the relative standard deviation is 3.45 %-5.43 %, which indicates that the enzyme biosensor has good detection characteristics.

3.2.4. Comparison of Detection Instruments

This thesis uses the detection instrument developed in this paper, the GDYN-303S rapid detection instrument pesticide residues produced by Jilin University-Little Swan Instruments Co. Ltd., and an Agilent Technologies 6890N gas chromatograph to detect pesticide residues in 8 types of vegetable samples, such as tomatoes, which were collected from three supermarkets under the administration of the Zibo vegetable basket product quality supervision and inspection center. The results are shown in Table 4.

Note: + indicates a "check out" (exceeding the national limit standard); -- indicates "not detected" (not exceeding the national limit standard).

The detected data for the detection instrument developed in this paper, the GDYN-303S rapid detection instrument pesticide residues produced by Jilin University-Little Swan Instruments Co. Ltd., and the Agilent Technologies 6890N gas chromatograph were compared. The results show that the detection instrument developed in this paper is simple and practical. It has the advantages of having a fast detection speed, low detection limit, accurate detection result, and zero probability of missed results. Compared to the options outlined in the literature [29], this instrument accelerates the speed of pesticide residue detection, and it assists in the general detection of pesticide residues within the production link, circulation link and sales link. It can also be used to supervise and inspect the safety and quality of agricultural products in a comprehensive way and improve the safety level of agricultural products. The combination of pesticide residue detection and laboratory detection was achieved, the dependence on large-scale analytical instruments was reduced, and the testing cost was reduced.

4. Conclusions

This design creatively replaces common electrodes with SPCE. The immobilization and modification of AChE on electrodes are studied. Without sample pretreatment, the detection speed, sensitivity and stability are improved.

The acquisition, conversion and amplification of weak electric signals by an AChE biosensor were studied here. An organophosphorus pesticide detection circuit system with high precision and high stability has been designed and developed. It is easy to operate and low in cost, and thus it will be easy to promote.

The wireless data transmission function of the detection instrument increased, and the detected data

were uploaded to the website of the traceability system for addressing agricultural product quality and safety in real time. The on-line analyses of pesticide residues in fruits and vegetables were completed, which will lay the foundation for the safe traceability of agricultural products.

Table 1. Actual detection data for pesticides at different concentrations.
(Materials: MWCNTs, CHIT, SnO_2, Nafion, SPCE, AChE, vegetables and fruits, standard concentrations of pesticides, and phosphate-buffered saline. Methods: enzyme-inhibition method and sol gel method. pH: 7.5. Scan rate: 0.05 V/s. Temperature condition: room temperature).

Sequence number	Pesticide residue concentration (μg/L)	Actual detectable quantity (μg/L)
1	0.02	0
2	0.04	0.03
3	0.05	0.05
4	0.1	0.12
5	1	1.08
6	10	10.12
7	100	99.85

Table 2. National standards for pesticide residues (part).

Sequence number	Common name for pesticides	Name of agricultural and sideline products	Maximum residue limit (MRL), ≤, mg/kg	National standard Number
1	2,4-Dichlorophenoxyacetic acid	Vegetables	0.2	GB15194-1994
2	Chlorothalonil	Vegetables Fruits	1 1	GB14869-1994 GB14869-1994
3	Fenthion	Vegetables Fruits	0.05 0.05	GB4788-1994 GB4788-1994
4	Dichlorodiphenyltrichloroethane (DDT)	Vegetables Fruits	0.1 0.1	GB2763-1981 GB2763-1981
5	Dipterex	Vegetables Fruits	0.1 0.1	GB16329-1996 GB16329-1996
6	Dichlorvos	Vegetables Fruits	0.2 0.2	GB5127-1998 GB5127-1998
7	Anilazine	Vegetables	10	GB15194-1994
8	Carbosulfan	Citrus	2	GB16333-1996
9	Chlorpyrifos	Pome leaf vegetables	1 1	GB16333-1996 GB16333-1996
10	Parathion	Vegetables Fruits	Not Detected Not Detected	GB5127-1998 GB5127-1998
11	Carbendazim	Vegetables Fruits	0.5 0.5	GB14870-1994 GB14870-1994
12	Diazinon	Vegetables Fruits	0.5 0.5	GB14928.1-1994 GB14928.1-1994
13	Phosalone	Leaf vegetables	1	GB16333-1996
14	Flucythrinate	Vegetables Fruits	0.2 0.5	GB15194-1994 GB15194-1994
15	Carbaryl	Vegetables Fruits	2 2.5	GB14971-1994 GB14971-1994
16	Quinalphos	Citrus Vegetables	0.5 0.2	GB14928.10-1994 GB14928.10-1994
17	Dimethoate	Vegetables Fruits	1 1	GB5127-1998 GB5127-1998
18	Hexachlorocyclohexane	Vegetables Fruits	0.2 0.2	GB2763-1981 GB2763-1981

Table 3. Spiked recovery rate detection in actual samples.
(Materials: MWCNTs, CHIT, SnO_2, Nafion, SPCE, AChE, vegetables and fruits, standard concentrations of pesticides, and phosphate-buffered saline. Methods: enzyme-inhibition method and sol gel method. pH: 7.5. Scan rate: 0.05 V/s. Temperature condition: room temperature).

Sample	Additive amount (μg/L)	Detection quantity (μg/L)	Rate of recovery (%)	RSD (%) (n=3)
Cabbage	10	10.15	101.5	3.45
Lettuce	10	9.23	92.3	4.36
Leek	10	10.33	103.3	5.43
Pakchoi	10	8.93	89.3	4.25

Table 4. Results from the Zibo vegetable basket product quality supervision and inspection center.
(Materials: MWCNTs, CHIT, SnO_2, Nafion, SPCE, AChE, vegetables and fruits, tomatoes, long beans, lettuce, rape, celery, cucumber, eggplants, peppers, standard concentrations of pesticides, and phosphate-buffered saline. Methods: enzyme-inhibition method, sol gel method, gas phase detection, and advanced instrument detection method. pH: 7.5. Scan rate: 0.05 V/s. Temperature condition: room temperature).

Test item Detection instrument type	Tomato	Long bean	Lettuce	Rape	Celery	Cucumber	Eggplant	Pepper
The detection instrument developed in this paper	--	+	--	--	--	--	--	--
GDYN-303S rapid detection instrument pesticide residues	--	+	--	--	--	--	--	--
Gas chromatograph	--	+	--	--	--	--	--	--

Acknowledgments

This work was supported by Special Project of Independent Innovation of Shandong Province (2018CXGC0214), Shandong Provincial Natural Science Foundation (ZR2019MC063), Key Innovative project for 2018 Major Agriculture Application Technology of Shandong Province School and City Integration Development Project of Zibo (2018ZBXC342, 2018ZBXC323), Ministry of Education of the People's Republic of China project on cooperation in production and education (201802362010).

References

[1]. A. N. O. Jardim, E. D Caldas, Brazilian monitoring programs for pesticide residues in food - Results from 2001 to 2010, *Food Control,* Vol. 25, 2012, pp. 607-616.

[2]. J. Sherma, Tuzimski T, High Performance Liquid Chromatography in Pesticide Resi-dueAnalysis, *Taylor & Francis Group*, New York, 2015.

[3]. E. S. Sousa, L. Pinto, M. C. U. D. Araujo, A chemometric cleanup using multivariate curve resolution in liquid chromatography: Quantification of pesticide residues in vegetables, *Microchem*, Vol. 134, 2017, pp. 131-139.

[4]. S. Hrouzková, M. Brišová, A. Szarka, Development of fast, efficient and ecological method employing vortex-assisted dispersive liquid–liquid microextraction combined with fast gas chromatography–mass spectrometry for pesticide residues analysis in alcohol-content samples, *Chromatogr. A*, Vol. 1506, 2017, pp. 18-26.

[5]. E. Matisová, S. Hrouzková, Analysis of endocrine disrupting pesticides by capillary GC with mass spectrometric detection, *Int. J. Env. Re.s and Pub. He,* Vol. 09, 2012, pp. 3166-3196.

[6]. M. A. Farajzadeh, A. Asghari, B. Feriduni, An efficient, rapid and microwave-accelerated dispersive liquid-liquid microextraction method for extraction and pre-concentration of some organophosphorus pesticide residues from aqueous samples, *Food Compos Anal,* Vol. 48, 2016, pp. 73-80.

[7]. P. Sivaperumal, P. Anand, L. Riddhi, Rapid determination of pesticide residues in fruits and vegetables, using ultra-high-performance liquid chromatography/time-of-flight mass spectrometry, *Food Chem*, Vol. 168, 2015, pp. 356-365.

[8]. G. Zhao, X. Sun, YM. Guo, et al., A Portable Instrument Based on Acetylcholinesterase Biosensor for the Rapid Detection of Pesticides Residues, *Sensors & Transducers* ,Vol. 182, Issue 11, November 2014, pp. 1-9.

[9]. M. A. Farajzadeh, M. R. Afshar Mogaddam, A. S. Rezaee, et al, Application of elevated temperature-dispersive liquid-liquid microextraction for determination of organophosphorus pesticides residues in aqueous samples followed by gas chromatography-flame ionization detection, *Food Chem,* Vol. 212, 2016, pp. 198-204.

[10]. F. Yong, T. Wen, P. Fei, et al., Simultaneous determination of pesticide residues and antioxidants in blended oil using a liquid-liquid extraction combined with dispersive solid phase extraction method, *Food Chem,* Vol. 229, 2017, pp. 347-353.

[11]. Z. Liu, P. Qi, X. Wang, et al, Multi-pesticides residue analysis of grains using modified magnetic nanoparticle adsorbent for facile and efficient clean up, *Food Chem*, Vol. 230, 2017, pp. 423-431.

[12]. X. S. Guo, X. Y. Zhang, et al. Developing a novel sensitive visual screening card for rapid detection of

pesticide residues in food, *Food Control,* Vol. 30, 1, 2013, pp. 15-23.
[13]. Y. C. Jiao, W. J. Hou, J. Y. Fu, et al. A nanostructured electrochemical aptasensor for highly sensitive detection of chlorpyrifos, *Sensor Actuat B: Chem,* Vol. 243, 2017, pp. 1164-1170.
[14]. J. Du, Research progress in detection methods of organophosphorus pesticide residues in fruits and vegetables, *Guangdong Chemical Industry,* Vol. 03, 2012, pp. 149-150.
[15]. X. Li, Q. Dong, Advances in the detection technique of organophosphorus pesticide residues, *Food and Nutrition in China,* Vol. 04, 2010, pp. 12-15.
[16]. X. H. Gao, Rapid detection of pesticide residues in vegetables is imperative, *Pesticide Science and Management,* Vol. 21, 1, 2000, pp. 16-17.
[17]. J. Yoon, T. Lee, G. B. Bapurao, et al, Electrochemical H_2O_2 biosensor composed of myoglobin on MoS2 nanoparticle-graphene oxide hybrid structure, *Biosens Bioelectron,* Vol. 93, 2017, pp. 14-20.
[18]. Z. Sun, L. Tian, M. Guo, et al, A double-film screening card for rapid detection of organophosphate and carbamate pesticide residues by one step in vegetables and fruits, *Food Control,* Vol. 81, 2017, pp. 23-29.
[19]. D. F. Chen, Research on acetylcholinesterase biosensor based on screen-printed electrodes, *Shandong University of Technology*, 2015.
[20]. Z. L Chen, Study on three zz-p-linked immunoassay and kit, Master's thesis, *Hangzhou: Zhejiang University,* 2006.
[21]. M. A. Dalviea, E. Sinanovicb, L. Londona, E. Cairncrossc, A. Solomond, H. Adamd, Cost analysis of ELISA, solid-phase extraction, and solid-phase microextraction for the monitoring of pesticides in water, *Environ Res,* Vol. 98, 1, 2005, pp. 143-150.
[22]. T. F. Sun, Enzyme-Linked Immunosorbent Assay and Application in Pesticide Residues Analysis, *Journal of Anhui Agricultural Sciences,* Vol. 38, 22, 2010, pp. 11981-11983.
[23]. X. Sun, W. P. Zhao, Z. H. Liu, et al, Preparation of acetylcholinesterase biosensor based on functionalized multiwalled carbon nanotubes, *Food Sci,* Vol. 33, 4, 2012, pp. 282-286.
[24]. F. C. Moraes, L. H. Mascarq, S. A. S. Machado, et al, Direct electrochemical determination of carbaryl using a multi-walled carbon nanotube/cobalt phthalocyanine modified electrode, *Talanta*, Vol. 79, 5, 2009, pp. 1406-1411.
[25]. S. G. Wang, J. He, H. Y. Yuan, et al, Study on immobilized enzyme carrier of enzyme biosensor, *Chem Sensor,* Vol. 24, 4, 2004, pp. 30-35.
[26]. F. X. Wei, J. Han, Q. Z. Liu, et al, Determination of acetylcholinesterase activity by chronoamperometry, *J Anal Sci,* Vol. 20, 6, 2004, pp. 663-664.
[27]. P. Sivaperumal, P. Anand, L. Riddhi, Rapid determination of pesticide residues in fruits and vegetables, using ultra-high-performance liquid chromatography/time-of-flight mass spectrometry, *Food Chem,* Vol. 168, 2015, pp. 356–365.
[28]. A. F. Mir, R. A. M. Mohammad, R. A. Samaneh, N. Nina, B. Mahdi, Application of elevated temperature-dispersive liquid-liquid microextraction for determination of organophosphorus pesticides residues in aqueous samples followed by gas chromatography-flame ionization detection, *Food Chem,* Vol. 212, 2016, pp. 198–204.
[29]. Z. W. Sun, L. Y. Tian, M. Guo, X. T. Xu, Q. Li, H. B. Weng, A double-film screening card for rapid detection of organophosphate and carbamate pesticide residues by one step in vegetables and fruits, *Food Control,* Vol. 81, 2017, pp. 23-29.

Published by International Frequency Sensor Association (IFSA) Publishing, S. L., 2019 (http://www.sensorsportal.com).

IFSA
Open Access Book
Advances in Measurements and Instrumentation: Reviews
Sergey Y. Yurish, Editor
1

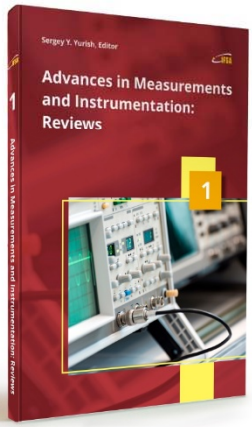

'Advances in Measurements and Instrumentation: Reviews', Book Series, Vol. 1 is covering some aspects related to metrology, sensors, measuring systems and sensor instrumentation as well as modeling and mathematical tools for measurements in a quality control and other applications. The book volume contains seven chapters written by nine contributors from academia and industry from 6 countries: Algeria, Canada, China, Germany, Slovak Republic and United Kingdom.

'Advances in Measurements and Instrumentation: Reviews' will be a valuable tool for those who involved in research and development of various measuring instruments and systems.

http://www.sensorsportal.com/HTML/BOOKSTORE/Advances_in_Measurements_Vol_1.htm